Magnetic Resonance Imaging 56 (2019) 3–13

Contents lists available at ScienceDirect

Magnetic Resonance Imaging

journal homepage: www.elsevier.com/locate/mri

Review article

NMR diffusometry with guest molecules in nanoporous materials

Seungtaik Hwang, Jörg Kärger*

Faculty of Physics and Earth Sciences, Leipzig University, Leipzig, Germany

A B S T R A C T

Application of pulsed field gradient (PFG) NMR to studying molecular diffusion in beds of nanoporous materials has given rise to novel insights and paradigm shifts in our understanding, which are reviewed in the present contribution. This gain in information is, in particular, related to the ability of PFG NMR to discriminate between various mechanisms affecting mass transfer in such systems. Examples include, inter alia, the sensitivity of PFG NMR toward transport enhancement in pore hierarchies as well as toward transport resistances acting, in addition to the diffusional resistance of the genuine pore space, either on the crystal surfaces or in their interior.

1. Introduction

As an omnipresent and fundamental phenomenon in nature, diffusion is of central importance for transport of the constituents of matter, namely, atoms and molecules [1–3]. Among the existing, non-invasive measuring techniques for investigating molecular diffusion, such as conventional uptake and release measurements [4–6] (including zero length column (ZLC) [7,8] and frequency-response [9–11] techniques as refined variants), permeation studies [12–14], quasi-elastic neutron scattering (QENS) [15,16], interference microscopy [17,18] and infrared microscopy [19–21], it was in particular the pulsed field gradient technique of nuclear magnetic resonance (PFG NMR – also referred to as pulsed gradient spin-echo (PGSE) NMR, NMR diffusometry and *q*-space imaging) [22,23] which proved to be an especially powerful technique. It has occupied, correspondingly, a most decisive role in diffusion studies, ranging from unconstrained molecular diffusion in liquids [24–27] to mass transfer of guest molecules in host porous materials [28–31] and in biological systems [32–34].

In particular, convincing demonstrations of the applicability of the PFG NMR technique to zeolites [30,35–38] have secured its firm foothold in studies of molecular self-diffusion in the intracrystalline pore system of zeolite crystallites. One of the major breakthroughs in the studies was that PFG NMR initiated a dramatic paradigm shift in the interpretation of the intracrystalline diffusion in zeolites by proving that a substantial discrepancy existed between the zeolitic diffusivity obtained by PFG NMR and the corresponding diffusivity deduced from conventional sorption experiments [39]. This discrepancy is due to the fact that the sorption measurements are based on the observation of molecular uptake by crystals, whose rate is affected by not only the intracrystalline diffusivity but also the permeability of the molecules through the crystal surface. If this latter effect is not taken into account and data analysis is performed solely under the implication of diffusion limitation, the sorption experiments do indeed give rise to an intracrystalline diffusivity lower than its genuine value measured by PFG NMR in which the influence of structural surface resistances is excluded [40].

The present review narrates the history of how PFG NMR, based on its ability to provide clear and direct evidence of quite a number of transport-related quantities, did finally succeed in accomplishing the paradigm shift in our understanding of mass transfer in zeolites and other nanoporous materials. The options for gaining deeper insights are shown to continue to exist up to the present. They are exemplified with the challenges provided by diffusion in hierarchically organized porous materials and the options of PFG NMR for, once again, providing insights into the phenomena determining intrinsic mass transfer in such novel materials which, so far, have remained inaccessible by any other measuring techniques.

2. Diffusion in beds of nanoporous crystallites

2.1. The “various” diffusivities

As a most important feature of the application of PFG NMR to beds of nanoporous crystallites, it has to be recognized that the type and the magnitude of diffusivities significantly depend on molecular displacements and, hence, on the size of the crystals under study. In other words, depending on the chosen observation time and measuring temperature, the molecular displacements will vary significantly, and the length of the mean diffusion path relative to the size of the crystals will decide which type of diffusion gives rise to the observed NMR data. In principle, three regimes of diffusion can be observable: intracrystalline diffusion, restricted diffusion and long-range diffusion.

* Corresponding author at: Faculty of Physics and Earth Sciences, Leipzig University, Linnéstrasse 5, 04103 Leipzig, Germany.
E-mail address: kaerger@physik.uni-leipzig.de (J. Kärger).

https://doi.org/10.1016/j.mri.2018.08.010
Received 26 July 2018; Received in revised form 20 August 2018; Accepted 23 August 2018

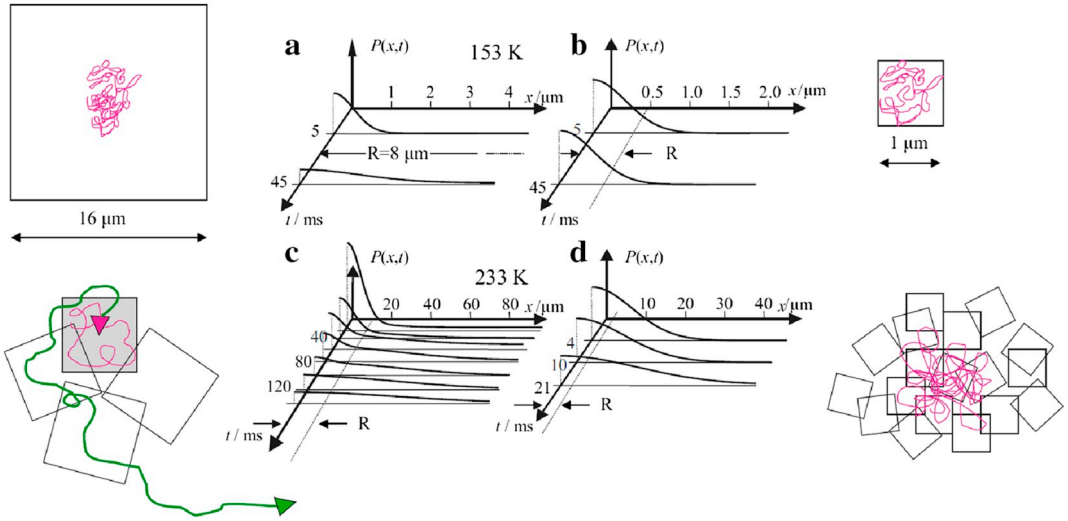

Fig. 1. Joint scheme of the mean propagators visualizing the diffusion paths of ethane molecules in beds of zeolite crystallites (type NaCaA) of different sizes (radius R) at 153 K and 233 K. The measurements are carried out in equilibrium conditions.
(Source: Reproduced from Ref. [44] with permission from the Royal Society of Chemistry).

One has, correspondingly, to distinguish between the three types of diffusivities by adapting the Einstein equation $D_{eff} = \langle r^2(t)\rangle/(6t)$ for correlating the (effective) diffusivity with the mean square displacement and the observation time.

As a convenient means of representing the regimes, the concept of mean propagator [41–43] can be employed. It is based on the well-known Stejskal-Tanner equation [22] correlating the local propagator and the probability distribution of molecular locations with the PFG NMR signal attenuation. It results from Fourier transformation of the signal attenuation and represents the probability that an arbitrarily selected molecule within a sample has traveled a distance x – typically micrometers – during a certain observation time t – typically milliseconds (in PFG NMR often referred to by the symbol Δ). The different regimes accessible in this way are illustrated in Fig. 1, which shows examples of the application of this formalism to ethane molecules in zeolites of type NaCaA.

In Fig. 1a, with large crystals at sufficiently low temperatures, intracrystalline diffusion can take place. This is a genuine intracrystalline diffusion within a homogeneous system since the molecular displacements are far longer than the pore diameters (thus indeed ensuring "random walk" of the guest molecules), but still much smaller than the crystal sizes. Fig. 1b shows restricted diffusion which may occur with small crystals at sufficiently low temperatures. In this case, most of the molecules are not able to overcome the energetic barrier to diffuse through the crystal surfaces (i.e. to get to the higher energetic level of molecules in the gas phase) and thus remain confined to the interior of the crystals in which they are accommodated. Therefore, the resulting diffusivity is exclusively determined by the size of the restricting volume and the observation time.

At sufficiently high temperatures, in Fig. 1d, the thermal energy is high enough to enable the molecules to leave the small, individual crystals and to diffuse through the whole batch, with interchanging periods of migration within and outside the crystals. This type of propagation is commonly referred to as long-range diffusion. This is exactly the situation under which M. Bourdart et al. have performed their measurements [45], with the mean diffusion path length of the water molecules exceeding the size of the zeolite crystals. The "effective" diffusivity probed by PFG NMR in this case, i.e. the long-range diffusivity $D_{\text{long-range}}$, is simply given by the product of the fraction of molecules outside the crystals p_{inter} and their diffusivity D_{inter}. This diffusivity may be very high, so that it overcompensates for the fact that the fraction p_{inter} is very small, giving rise to an overall diffusivity $D_{\text{long-range}}$ which, possibly, may even exceed the diffusivity in the liquid D_{liquid} [46,47].

With larger crystals considered in Fig. 1c, the information about the relative fraction of the molecules which have left the crystals after a given (observation) time can be acquired by distinguishing between the two constituents of the mean propagator. The narrow constituent at relatively small x corresponds to the molecules still staying within the crystals, while the broad one at larger x is brought about the molecules having left the crystals. The relative fraction of the molecules which have left the crystals is directly given by the area under the broad constituent and is seen to increase with increasing observation time t (Fig. 1c). Plotting this fraction is thus easily seen to provide information equivalent to that of tracer exchange between the interior and the surroundings of the crystals. Tracer exchange, however, is known to be affected by intracrystalline diffusion AND permeation through the crystal surface, different from the PFG NMR measurement performed under the conditions shown in Fig. 1a which is exclusively determined by intracrystalline diffusion. Having these two types of independent information, PFG NMR was able to identify the existence of "surface barriers" as the origin of the huge differences (up to five orders of magnitude!) between conventional and PFG NMR diffusion measurements with zeolites [39,48].

Zeolite crystals are industrially applied for, notably, matter upgrading by molecular sieving/separation and/or conversion, where they are commonly used as compacted particles consisting of numerous crystallites. For optimizing their performance, it is of crucial importance to be equipped with knowledge of the limiting processes of mass transfer, including the mechanisms of intracrystalline and long-range diffusions. This is exactly the type of information which can be provided by PFG NMR. As an example, we are going to refer to a PFG NMR diffusion study [49] performed with particles of industrial fluid catalytic cracking (FCC) catalysts, which consist of USY zeolite crystals (the catalytically active component, containing micropores) and a binder matrix (containing meso- and macropores). Fig. 2 shows, as a result of the study, the two different "types" of n-octane diffusivities, namely the intracrystalline diffusivity and the long-range ("intraparticle") diffusivity, in the FCC catalysts as a function of temperature. Since the measuring temperatures in PFG NMR are much lower than the range of the actual operating temperature in the industry, the data are simply extrapolated to higher temperatures. At a typical operating temperature of 600 °C, the intracrystalline diffusivity is expected to be lower than the intraparticle diffusivity. The relevant time

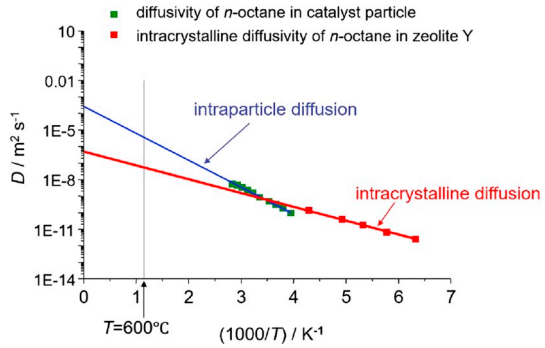

Fig. 2. *n*-Octane diffusion in fluid catalytic cracking (FCC) catalysts.
(Source: Reprinted with permission from Ref. [49]. Copyright 2005 American Chemical Society).

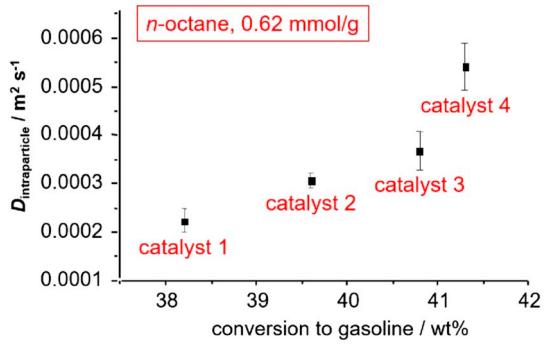

Fig. 3. Correlation between intraparticle diffusivities and catalytic performance.
(Source: Reprinted from Ref. [37], Copyright 2005, with permission from Elsevier).

constants, however, depend on not only the respective diffusivities (D) but also on the sizes (L) of the zeolite crystals and the catalyst particles (scaling as L^2/D which is easily seen to be the only way to combine these two parameters to a quantity with the dimension of time). Considering the size of the individual crystals, which is ca. 40 times smaller than that of the particles, the uptake times in the crystals should be much shorter than those in the whole particles. Therefore, the rate of the overall transport in the FCC catalysts, which determines the catalytic performance and hence the rate of gain of value-added products, is exclusively controlled by the rate of mass transfer through the catalyst particles, i.e. by the intraparticle diffusivity. Correspondingly, it is found that the overall catalytic performance in oil-to-gasoline process is enhanced with increasing intraparticle diffusivity as indicated by an increase in the oil-to-gasoline conversion in Fig. 3.

2.2. The two-region model

As an attempt to comprise the various situations under which PFG NMR diffusion studies may be performed and which are seen to appear with quite different patterns of the mean-propagator representations (Fig. 1), the formalism of the two-region model [50–52] was introduced already in the late 1960s. It is based on the assumption that the overall mass transfer in the system under study is described by the diffusivities D_i in the two regions, their relative populations p_i and the mean life times τ_i in either of them. Since the relative populations add up to 1 ($p_1 + p_2 = 1$) and are, moreover, subject to the detailed-balance condition $p_1/\tau_1 = p_2/\tau_2$, the dynamics in the two-region model is determined by four independent parameters. By introducing the mean life times it bears, inherently, the implication that, during the time interval dt, any molecule will get from its present region (i) to the other one with the probability dt/τ_i, i.e. independent of its history. One easily recognizes that this implication is not strictly fulfilled with the system under study if the intracrystalline pore space and the space between the crystals are understood as the two regions in this model. The probability that a particular molecule is able to leave its crystal does, obviously, significantly depend on its "history", namely on the diffusion path length that it has covered previously within the given crystal. Nevertheless, the two-region model has been found to serve as a useful first-order estimate, nicely reproducing – in at least a qualitative way – the situation in beds of zeolite crystallites [53] as well as in many more "compartmented" systems [54–60]. This is, in particular, true for biological tissues, where the role of "compartments" is assumed by the biological cells [61–64].

Accessible information enhances with the possibility of attaining separate NMR signals from the molecules accommodated in the two different regions [58,65]. On considering mass transfer in zeolites, such a possibility is indeed known to be provided by combining PFG NMR measurement with magic angle spinning (MAS) [66–68], as recently demonstrated [69] with the investigation of water diffusion in lithium-exchanged low-silica X-type zeolites [70,71].

Fig. 4 shows the two lines of water molecules which, in such a way, become observable. The lines at about 3.5 and 5.1 ppm refer, respectively, to the water molecules "trapped" in small cages within the

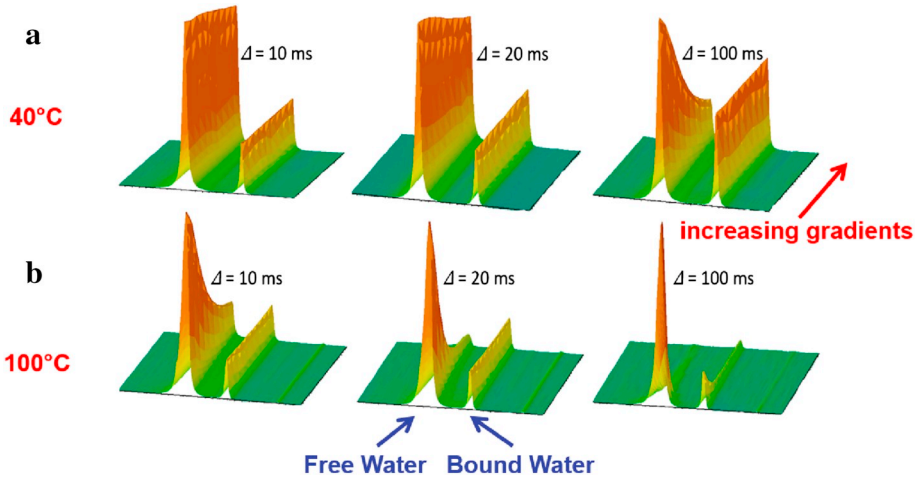

Fig. 4. Stack plots of the ^{1}H MAS PFG NMR signal attenuation for water in 100Li-LSX at 313 K (a) and 373 K (b) for the indicated observation times Δ. The field gradient amplitude increases from 0.011 T m^{-1} to 0.486 T m^{-1}.
(Source: Reprinted from Ref. [69], Copyright 2018, with permission from Elsevier).

zeolite structure (the so-called sodalite cages [72]) and to the remaining ones in the intracrystalline pore space which is in fast exchange both internally and, through the intercrystalline space, with also the other crystals. The sodalite cages accommodate about 5.6% of the total water content [73,74]. Measuring the NMR signals stemming from the two spaces separately is only possible owing to a combination of magic angle spinning (MAS) with PFG NMR which, ultimately, enables us to probe water exchange between the two regions. At a low temperature (Fig. 4a), the signal attenuation with increasing pulsed field gradient intensity exhibits an expected behavior: diffusion attenuation for the free water in the larger pores and no attenuation at all for the bound water in the tiny pores (in which only four water molecules are accommodated!). At a high temperature, however, the bound water molecules also show diffusion attenuation. Now, during the largest observation time considered, a notable fraction of the water molecules are obviously able to leave the small cages (Fig. 4b), being replaced by others coming from “outside”. They, correspondingly, have the chance of covering sufficiently large displacements giving rise to the observed signal attenuation.

By attributing the water molecules inside and outside the sodalite cages to the two regions we are, obviously, able to get rid of the limitation in the two-region model mentioned initially in this section. All the molecules in the sodalite cages may, as a matter of course, escape from there anytime with equal probability, and the probability that a molecule “from outside” may enter a sodalite cage is as well independent of its past, i.e. from the distance that it has covered on its diffusion path. As a further simplification we note that the diffusivity of the water molecules within the sodalite cages is known, that is, equal to zero.

Fig. 5 shows the result of the fitting procedure by a solution of the two-region model of PFG NMR, aiming to serve as an approach to the experimentally determined signal attenuation as a function of the pulsed field gradient intensity (here represented by the parameter q) shown in Fig. 4. It takes into account that one is able to separately record the signals stemming from the two regions with different properties of nuclear magnetic relaxation. The model calculations are seen to nicely reflect all major features of the experimental results. For the low temperature, the results of the simulation are even found to be in excellent agreement with the PFG NMR data (Fig. 5a and b). At the high temperature, however, systematic deviations for the freely diffusing water molecules become clearly visible (Fig. 5c). This limitation in accuracy is easily referred to the fact that mass transfer through the intra- and intercrystalline pore space is too complex for being adequately represented by a single diffusivity as required by the approach inherent to the two-region model.

2.3. Confinement by external and internal transport resistances

Under the conditions of the PFG NMR measurements as considered in Fig. 1b, the molecules are assumed to remain caught within the interior of the individual crystals. This may be brought about as a consequence of the potential energy step (being of the order of the heat of adsorption) which, at sufficiently low temperatures, results in a diminution of the probability of molecular jumps from the interior of the crystal into the surrounding gas phase to arbitrarily small values. The same effect is also attained by a total blockage of intercrystalline space (as achieved, e.g., in Ref. [75] by coating with silica). Under such conditions, for sufficiently long observation times (as implied in the case shown in Fig. 1b) the propagator becomes independent of time and, hence, of the mean square displacement (being nothing else than the squared distribution width or variance of the propagator). Via Einstein's relation, the PFG NMR diffusivity attained under such conditions is easily seen to decay, inversely proportional to time.

It is important to note that analytic expressions do as well exist for the short-time limit where the molecules start to “experience” their confinement by the surface of the crystals. This formalism has been developed by Mitra and co-workers [76,77] for the diffusion of molecules confined to a macropore. The developed formalism does even

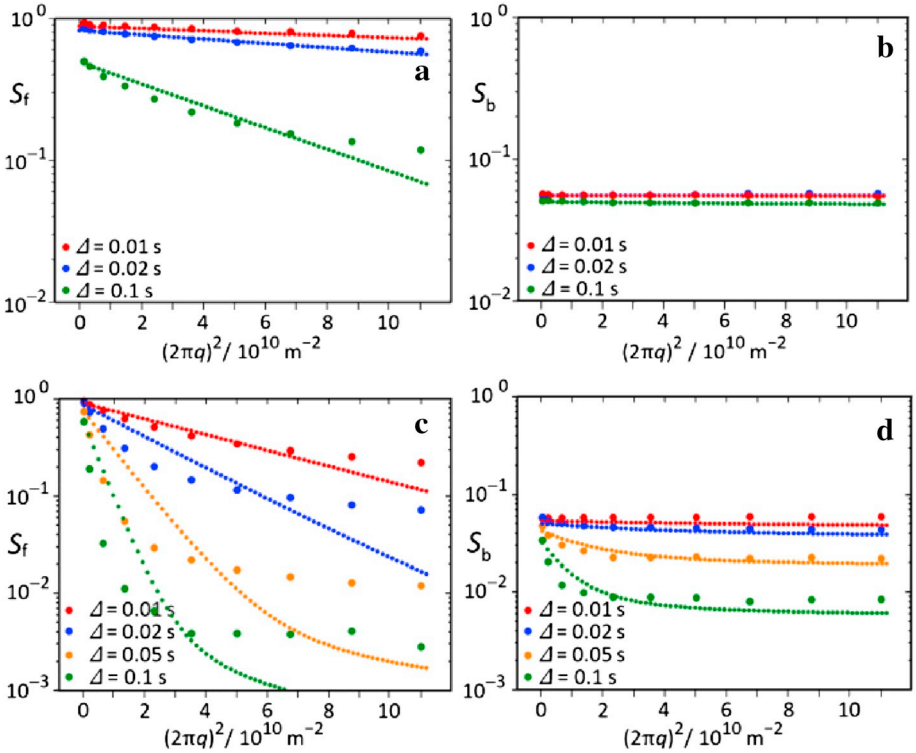

Fig. 5. PFG NMR signal attenuation plots for different observation times Δ as a function of the squared intensity q of the field gradient pulses: free water (a) and bound water (b) at 40 °C; free water (c) and bound water (d) at 100 °C.
(Source: Reprinted from Ref. [69], Copyright 2018, with permission from Elsevier).

offer the option of discriminating between "reflecting" (as so far considered) and "absorbing" boundaries. On considering *n*-hexane in zeolite NaX [78], with appropriately chosen particle sizes and measuring temperatures, the dependence of the diffusivities on the observation time were indeed found to follow the limiting case of reflecting boundaries in the Mitra formalism [76,77], even with an indication of the deviation from a linear square root dependence, predicted by the formalism as a second-order effect.

While the large hexane molecules are kept within the crystal as a consequence of their high heat of adsorption, thus indeed experiencing the crystal boundary as a reflecting barrier, the tetrafluoromethane molecules are observed to be small enough for leaving the crystals essentially anytime they have reached their external surface. The molecules which have left the crystals cover very large displacements and their contribution to overall signal attenuation (see Fig. 1c) is, therefore, easily to be distinguished from those within the crystals. It is thus easily possible to confine analysis to only those molecules which have never been in contact with the surface. This is the situation with the other limiting case of the Mitra formalism, considering "absorbing" boundaries where molecules, once they have reached the surface, do not contribute anymore to the signal.

Diffusion in beds of nanopores with no surface resistances and large long-range diffusivities are thus found to represent an alternative to the situation originally considered in the Mitra formalism, where signal loss on the surface (of the macropore) was associated with its high relaxivity. The validity of the formalism was confirmed by a satisfactory agreement between the PFG NMR data and the microscopically determined values of the crystal radius as appearing from Fig. 6. The values of the genuine intracrystalline diffusivities D_0 and the crystallite radii R, the two parameters obtained from the best fits of the Mitra formalism, are tabulated in Table 1.

After detecting the possibility that the mass transfer is significantly affected by the resistances on the external crystal surfaces, it comes as a big surprise to observe anomalies in the PFG NMR diffusivities even under conditions where they are supposed to coincide with the coefficients of genuine intracrystalline diffusion. Fig. 7 shows the results of such a study performed with zeolite crystals large enough in comparison with the recorded diffusion path lengths, so that the resulting diffusivities should be independent of the observation time [79]. This, however, is only the case with the largest temperature. One has to conclude, therefore, that the mass transfer in the interior of the individual crystals is also affected by transport resistances acting in addition to the diffusion resistance incurred by the genuine pore space itself. Increasing thermal energy of the guest molecules facilitates, with

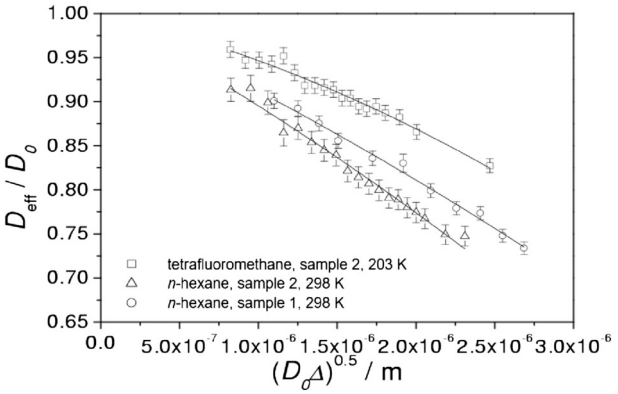

Fig. 6. Relative effective intracrystalline diffusivities $D(t)/D_0$ as function of $\sqrt{D_0 t}$ for *n*-hexane in the single-component sample (○), in the two-component sample (Δ), and for tetrafluoromethane in the two-component sample (□), respectively. The lines shown in the diagram represent the best fits of the Mitra formalism to the experimental data of $D(t)$ with D_0 and R as fitting parameters. (Source: Reprinted from Ref. [78], with the permission of AIP Publishing).

Table 1
Estimate of the genuine intracrystalline diffusivities D_0 and the crystal radii R by PFG NMR data analysis on the basis of the Mitra formalism.
(Source: Reprinted from Ref. [78], with the permission of AIP Publishing).

	D_0 ($m^2 s^{-1}$)	R (μm)
2 *n*-hexane/cav., single component adsorption, 298 K	3.53×10^{-10}	9.1
1 *n*-hexane/cav., two-component adsorption, 298 K	5.54×10^{-10}	7.8
1 tetrafluoromethane/cav., two-component adsorption, 203 K	4.17×10^{-10}	9.1

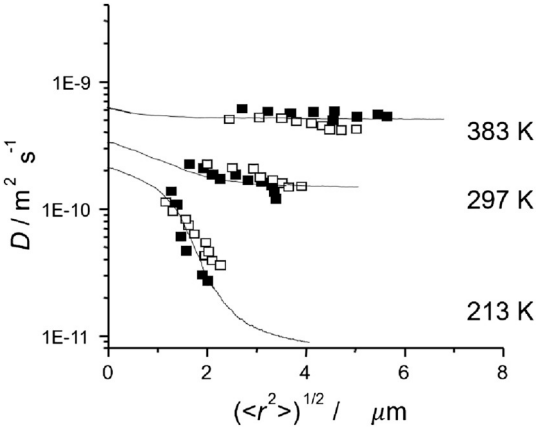

Fig. 7. Dependencies of the *n*-butane intracrystalline diffusivity on the root mean square displacements at different temperatures: the experimental data (points) and those obtained by dynamic Monte Carlo simulations (solid lines). (Source: Reprinted from Ref. [80], Copyright 2002, with permission from Elsevier).

rising temperature, overcoming these internal barriers: accordingly, at sufficiently high temperature, the mass transfer may in fact be expected to become unaffected by these barriers, yielding consistency of the recorded diffusivities with varying observation time. The validity of this reasoning has been confirmed by dynamic Monte Carlo simulations [80] which (based on quite simple assumptions on the resistances, namely a spacing of 3 μm and an activation energy of 21.5 kJ/mol) are found to exhibit perfect agreement with the experimental data, as indicated by the solid lines in Fig. 7. Today, confirmed by the information meanwhile obtained by also microspectroscopy [81–83], transmission electron microscopy [84] and comparison with QENS diffusion data (recorded with displacements of nanometer rather than micrometers) [85–87], the existence of such internal resistances is known to be more like a general rule rather than an exception.

The effects of both the confinement by external surfaces and the resistances at internal interfaces are clearly recognized in diffusion measurements of water molecules and lithium cations in hydrated zeolite Li-LSX [73]. The first (steep) and the second (moderate) slopes, in both Fig. 8a and b, correspond to the internal resistances and the external barrier, respectively, thereby revealing that there are two types of extra-resistances directly affecting the overall mass transport in the zeolite, in addition to the diffusional resistance of the genuine pore network [73]. These very first PFG NMR diffusion measurements with cations in zeolites, to the best of our knowledge, have opened a new field of research aiming at an in-depth study of cation locations and their variation with time within zeolites.

3. Diffusion in pore hierarchies

The functionality of nanoporous materials in their technological applications for matter upgrading by separation and selective conversion relies on the intimate contact between the guest molecules and the internal surface of the host materials. This intimate contact, typically

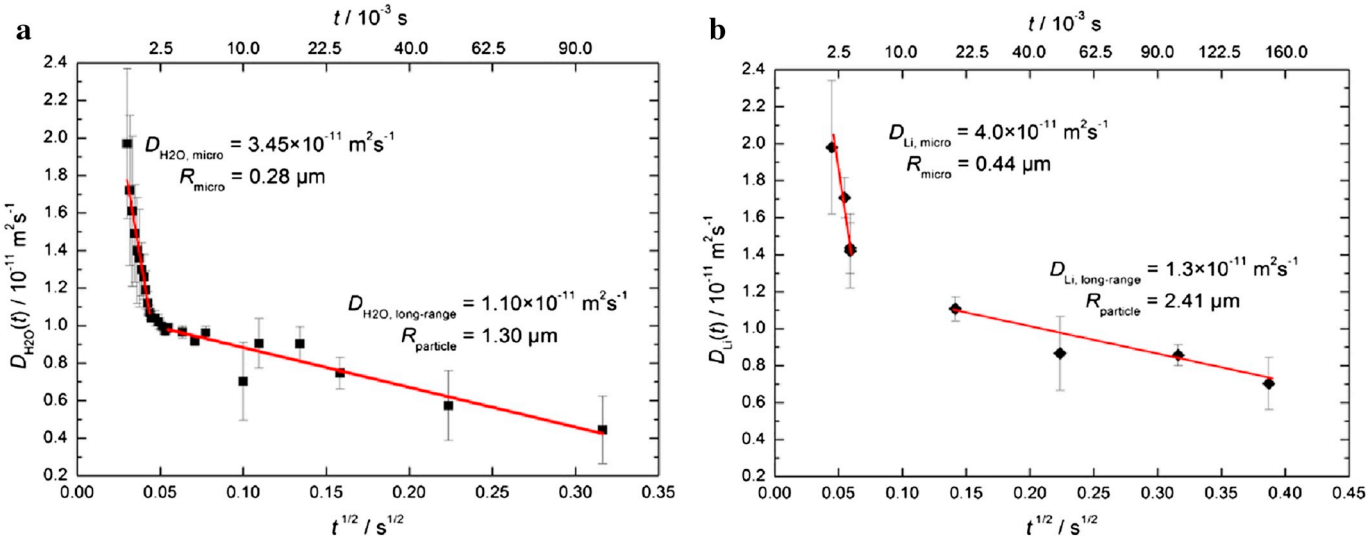

Fig. 8. Effective diffusivities of water (via ^{1}H PFG NMR) at 25°C (a) and of the lithium cations (via ^{7}Li PFG NMR) at 100 °C (b) in hydrated zeolite Li-LSX. (Source: Reprinted with permission from Ref. [73]. Copyright 2013 American Chemical Society).

ensured by the pore sizes close to the molecular diameters, tends to impede the translational mobility of the molecules in such systems. The gain in value-added products, however, can never be faster than allowed by the migration rate of the molecules. Small pore sizes of the host material as a prerequisite of functionality do thus, at the same time, restrain the performance by limiting the rates of molecular diffusion. The fabrication of materials possessing "hierarchical" pore spaces [88–92] has been recognized as a particularly promising option for overcoming this trade-off. In such materials, a homogeneous space of micropores (with pore dimensions in agreement with the required functionality in separation or conversion) is permeated by a network of mesopores, which ensures the sufficiently fast exchange between the particle interior and the surroundings. Accompanied with this increase in complexity, the number of parameters relevant for an accurate description of intrinsic mass transfer is also further increasing. We easily recognize the necessity of introducing at least four parameters. They coincide, most remarkable, with exactly those four independent parameters which we had already referred to in Section 2.2 considering the two-region model, namely, the diffusivities, the relative occupancies of the two pore spaces, and the exchange times (with only two of the latter four parameters being arbitrary). The two-region model may thus serve as a useful tool for an in-depth study of mass transfer in also hierarchically porous materials. In many cases, however, it will be sufficient to consider only the relevant limiting case [93,94]. We are going to refer to them in more detail in the subsequent section, based on the outcome of dynamic Monte Carlo simulations in an appropriately chosen model system. The following sections shall deal with the presentation and discussion of the results of PFG NMR diffusion measurements in "real" pore hierarchies.

3.1. Insights by dynamic Monte Carlo simulation

The top of Fig. 9 illustrates the model applied for simulating mass transfer in a hierarchical pore space [93,94]. It consists of a microporous continuum (top left), which is traversed by three arrays of parallel channels (to which we refer as transport pores or mesopores), perpendicular to each other (top right). Diffusion is simulated on a network of equally separated grid points. Jump rates on grid points in the transport pores are enhanced in comparison to those in the micropores, giving rise to correspondingly enhanced diffusivities. Exchange rates between the two pore spaces are chosen in correspondence with the respective populations.

This model has, in particular, been exploited for investigating molecular uptake and for correlating the patterns of guest distributions with the rate-determining phenomena (and parameters) of mass transfer during uptake. Molecular uptake is simulated by starting with an empty lattice. Equilibrium with the surrounding atmosphere is ensured by keeping, after each simulation step, the fraction of occupied grid points in the surface layer constant. The bottom of Fig. 9 shows two typical patterns of guest distribution obtained as snapshots during the simulation runs of molecular uptake. Both refer to identical partial loadings. Depending on the parameters chosen for describing the internal mass transfer they show, however, distinctly different patterns.

In the representation on the bottom left we recognize that the molecular uptake occurs essentially homogeneously all over the crystal. This exemplifies the limiting case of "slow exchange" where diffusion in the transport (the meso-) pores is very fast in comparison with uptake by the micropores. The space of mesopores is therefore filled by guest molecules long before a significant portion of the micropores has been occupied. Uptake occurs, as a consequence, over essentially the whole of the internal surface of the mesopores. Its rate is thus determined by the diffusivity in (exclusively!) the micropores. However, the diffusion pathways to be covered for sample filling are now, owing to the presence of the mesopores, notably reduced. They may be shown [93,94] to scale with the total volume of the microporous space divided by the total area of the interface between the micro- and mesoporous spaces.

The representation on the bottom right depicts the opposite situation where "fast exchange" between the meso- and microporous spaces gives rise to the formation of a diffusion front. It propagates from the external particle surface toward its interior as it is the case with also the purely microporous host material. This means that it is still the particle size which determines the diffusion path lengths to be covered during the molecular uptake or release. The effective diffusivity, however, is now given by the combined effect of mass transfer in the micro- and mesopores. The situation reminds of the regime of long-range diffusion referred to in already Section 2.1 considering mass transfer through beds of nanoporous crystals. Now, however, deviating from the situation with beds of nanoporous particles, the microporous space forms a continuum, so that mass transfer in both pore spaces contributes to the overall molecular uptake (or release). The effective diffusivity, correspondingly, results as the weighted mean of the (effective) diffusivities in the two pore spaces: $D_{\mathrm{eff}} = p_{\mathrm{micro}}D_{\mathrm{micro}} + p_{\mathrm{meso}}D_{\mathrm{meso}}$. Note that, as a consequence of the presence of the mesopores, D_{micro} may notably differ from D_{intra} measured in the purely microporous specimen. We are going to experimentally show this case in the subsequent sections dealing with the results PFG NMR diffusion studies in hierarchically organized

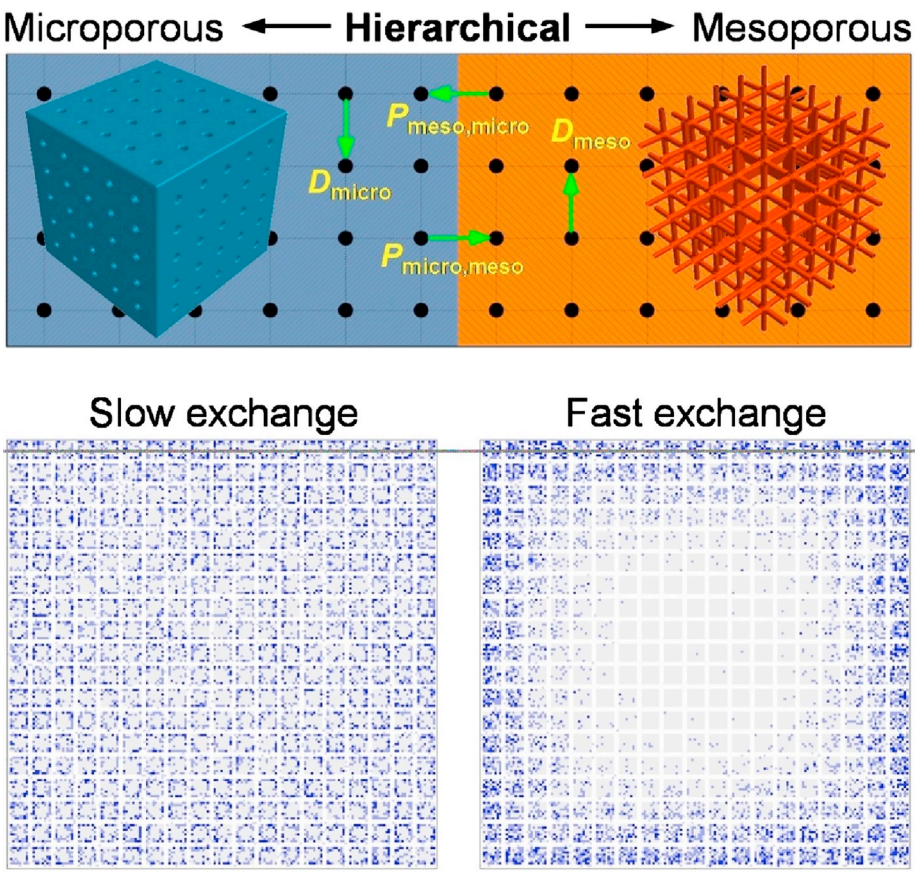

Fig. 9. Model system applied for simulating mass transfer: microporous continuum (top left) and arrays of mesopores (top right). Distributions of guest molecules in the modelled grid in the limiting cases of slow exchange (bottom left) and fast exchange (bottom right). The purely microporous body (small squares) is percolated by a network of mutually intersecting mesopores (equidistant channels).
(Source: Reproduced from Ref. [93], with permission from John Wiley and Sons).

pore spaces.

Mass transfer in hierarchically porous materials is thus seen to indeed depend on a number of parameters. There are, however, quite different possibilities of how the overall mass transfer is affected by these parameters. It has been visualized that, e.g., under the conditions of "fast exchange", uptake and release rates (as the key numbers of mass transfer) vary with the particle size which is not the case under "slow exchange" conditions. Though a sufficiently high diffusivity in the mesopores is clearly a prerequisite for the limiting case of slow exchange, once established, molecular uptake and release under slow exchange conditions are controlled by the diffusion rate in exclusively the micropores. Uptake and release under fast-exchange conditions, however, are affected by the diffusivities in both pore spaces. Comprehensive knowledge about the governing phenomena of mass transfer in hierarchically porous materials is thus considered quintessential to design their optimum applications. Therefore, the development of effective strategies for their determination by reliable experiments has become a hot topic of current research [95] along with particular challenges for PFG NMR diffusion measurements [96–99] – some of which we are now going to refer to in more detail.

3.2. PFG NMR diffusion measurements in mesoporous zeolites

The enhancement of the overall mass transfer due to the presence of mesopores is experimentally observed in PFG NMR diffusion measurements of short *n*-alkanes in zeolite NaCaA [100,101]. In comparison with the propane diffusivities in the purely microporous space, its effective diffusivity in the hierarchical pore system possessing both micropores and intentionally added mesopores is seen to increase by several orders of magnitude, showing the largest diffusivities for the largest mesopore content. The diffusivities shown in Fig. 10 are plotted as a function of the observation time. Their constancy confirms that only normal diffusion has occurred, with the covered displacements between 200 nm and 10 μm.

While the great benefit of the mesopores was immediately visible with propane, the situation becomes much more complex when considering ethane as a guest molecule (in the very same zeolite NaCaA [101]), as illustrated by Fig. 11. This difference in the patterns must be referred to the smaller critical diameter of ethane in comparison with propane. Although the difference in the diameters is in fact quite subtle, their similarity with the pore sizes is known [86,102,103] to give rise to an enhancement of the diffusivity of ethane in zeolite NaCaA in comparison with propane by more than two orders of magnitude. This dramatic increase does as well increase, for ethane, the contribution of micropore diffusion to the overall ("effective") diffusivity.

At low temperatures, the diffusivities in the mesoporous zeolites are even found to be below those in the purely microporous ones. This is due to the fact that, given their low occupancy at low temperatures, the mesopores act as obstacles rather than as highways of mass transfer. Exactly to such a situation we did refer already at the end of Section 3.1, highlighting the difference between D_{micro} and D_{intra}. The validity of this reasoning, i.e. mesopore hindrance to diffusion, is evidenced by comparison of the diffusivities in zeolites with "open" mesopores (represented by open symbols in Fig. 11) and those with blocked mesopores (filled symbols). At sufficiently low temperatures both diffusivities are indeed found to essentially coincide. Only at the highest temperatures considered, the fraction of molecules in the mesopores becomes large enough, so that the presence of the mesopores leads to an increase in the diffusivity in comparison with the purely microporous zeolites. The dashed line in Fig. 11 (with the slope given by the isosteric heat of adsorption) serves only as a guide to the eye, indicating the increase in pressure and, hence, in the relative amount p_{meso} of molecules in the mesopores with increasing temperature where it is taken into account that the relative number of molecules in the gas phase of the (fused) PFG NMR sample tubes remains negligibly small in comparison with the amount adsorbed. The increase in the experimentally

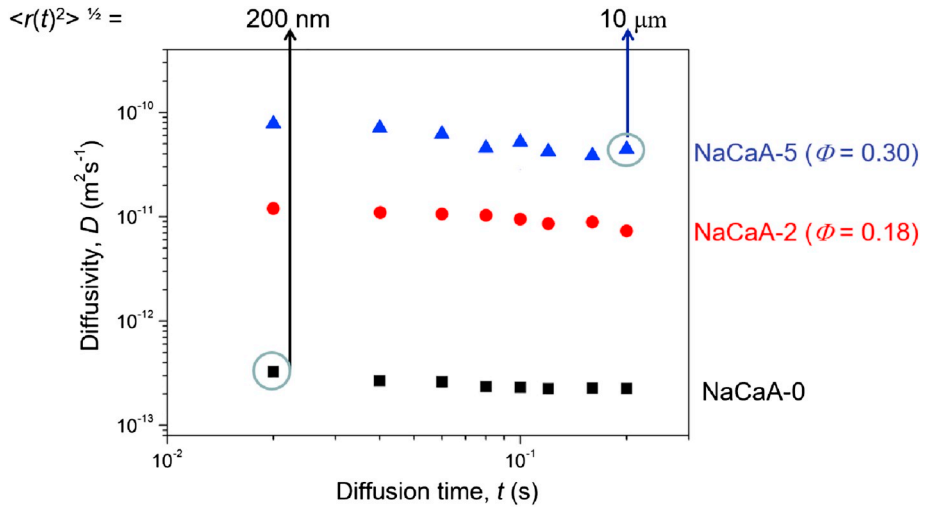

Fig. 10. Self-diffusivities of propane in zeolite NaCaA at 25 °C. Squares: purely microporous; Circles: mesoporous with a volume fraction $\phi = 0.18$; Triangles: mesoporous with a volume fraction $\phi = 0.30$.
(Source: Reproduced from Ref. [100], with permission from John Wiley and Sons).

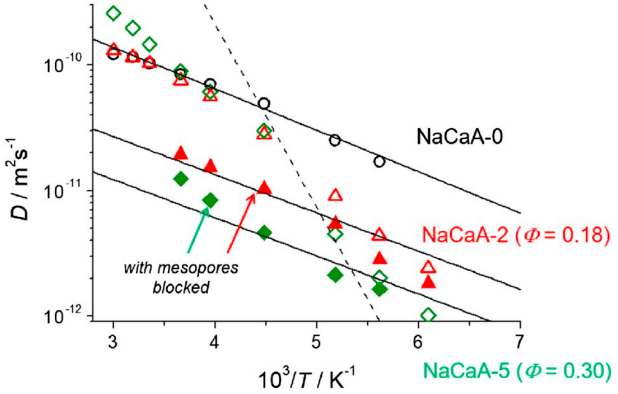

Fig. 11. Arrhenius plot of ethane self-diffusivities in zeolite NaCaA. Open circles: purely microporous; Open triangles: open mesopores with a volume fraction of 0.18; Filled triangles: blocked mesopores with a volume fraction of 0.18; Open diamonds: open mesopores with a volume fraction of 0.30; Filled diamonds: blocked mesopores with a volume faction of 0.30. The dashed line is a guide to the eye, representing the variation of the contribution of diffusion in the (unblocked) mesopores to the overall intracrystalline diffusivity with varying temperature.
(Source: Reprinted from Ref. [101], Copyright 2012, with permission from Elsevier).

determined diffusivities is seen to remain far below this estimate, evidencing the substantial contribution of micropore diffusion to overall mass transfer under even these conditions.

To the best of our knowledge, most of the PFG NMR diffusion studies performed with hierarchical materials have been carried out under the fast exchange conditions. This is a consequence of the fact that, for ensuring sufficiently large observation times together with the application of sufficiently strong field gradient pulses, only systems of high internal mobility (and with, correspondingly, large transverse nuclear magnetic relaxation times) have been considered. Molecules are thus in general found to repeatedly switch between the two pore spaces. It has been demonstrated in Section 2.2 with the water molecules captured by the sodalite cages that the combination of MAS and PFG NMR may eventually transcend this limitation.

3.3. PFG NMR diffusion measurements in hierarchically porous silica

Novel opportunities and challenges for PFG NMR diffusion studies with pore hierarchies have opened up with the advent of materials with hierarchically arranged meso- and macropores. Fig. 12a shows, as an example, the scanning electron micrograph of an hierarchically porous silica monolith [104,105] consisting of a mesoporous bulk phase traversed by macropores. With due precautions, PFG NMR is able to trace mass transfer in three different scenarios as illustrated by Fig. 12b–d [106]. The situation shown in Fig. 12b is attained by appropriately choosing the measuring temperature above the melting point in the mesopores, but below that in the macropores [107–110]. Slight temperature enhancement leads to melting all over the sample and, thus, to scenario (d). In fact, this scenario may even be maintained due to "supercooling" [111,112] by, once again, carefully cooling down [113]. As a consequence, all measurements can be implied to be performed at an essentially identical temperature of 273 K. Similarly, scenario (c) is attained with, again, a supercooled probe liquid (at 273 K), but now in the monolithic macroporous silica in which the mesopore structure is not present due to the omission of postgelation treatments [114].

Fig. 12e provides an overview of the diffusivities attained in the three scenarios considered, in comparison with the diffusivity in the bulk liquid. As the most remarkable feature, the diffusivity under condition (b) is observed to be quite significantly (by a factor of about 6) reduced, while diffusion in exclusively the macropores (c) and under fast exchange conditions (d) are only slightly (by a factor of about 1.5) below the bulk diffusivities. The latter finding is not unexpected since the material under study has, among others, been designed for application in chromatography [115,116] where high throughputs and, correspondingly, low resistances by tortuosity are intended. On search for the origin of the dramatic reduction of the diffusivity in solely the mesopores (i.e. under condition b) we note that the mean diffusion path lengths of the guest molecules as given on the abscissa in Fig. 12e are comparable with or do even notably exceed the spatial extensions of the purely mesoporous pore space which appear from the scanning micrographs in Fig. 12a. The diffusional resistance, to which the guest molecules are subject, is therefore caused by both the mesopore tortuosity and by the tortuosity brought about by the finite extension of the mesoporous pore space. We are thus encountering a situation to which we referred already in the context of Fig. 11 where total blockage of one pore space (there it was the mesopore space) was observed to notably reduce the diffusivity in also the complementary pore space [117].

The reduction in diffusivity is, in scenario (b), caused by the blockage of the macropores and does, correspondingly, not exist anymore under the fast-exchange conditions as considered in Fig. 12d. The

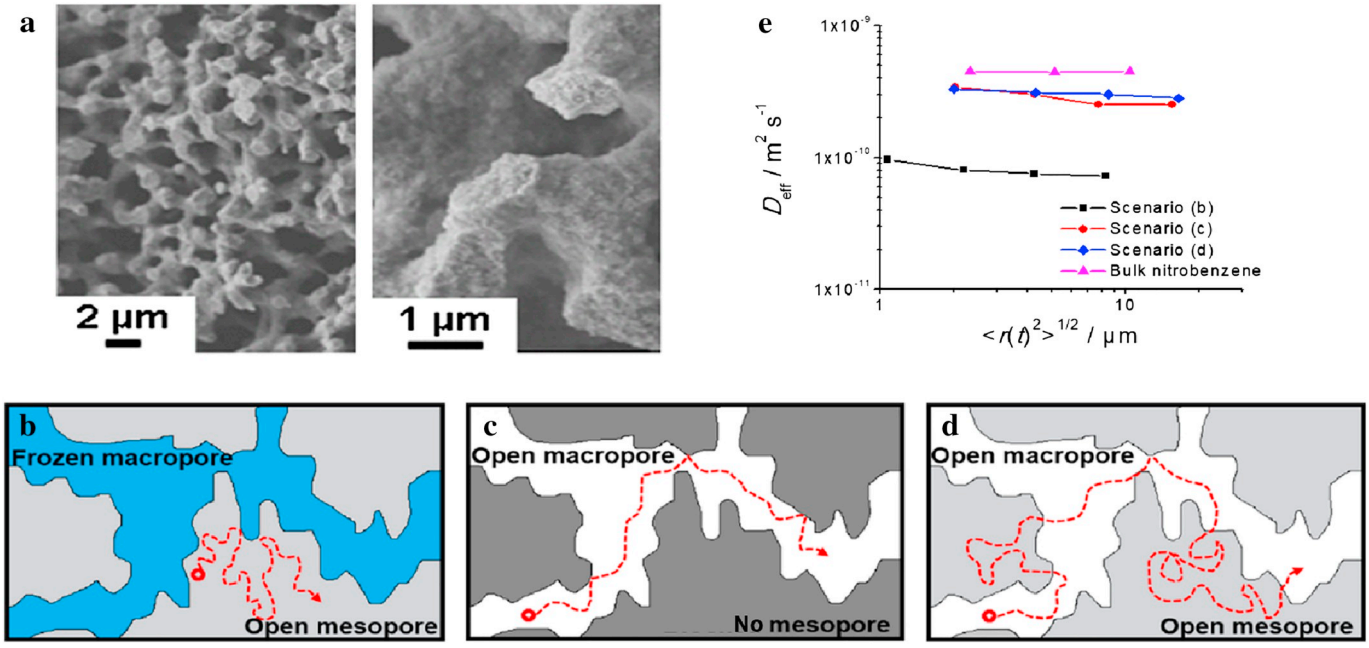

Fig. 12. PFG NMR measurement of guest diffusion (nitrobenzene) in hierarchically porous silica: (a) SEM image of the host material. (b–d) The different scenarios of mass transfer considered. (e) The resulting diffusivities in comparison with the free liquid, plotted as a function of the root mean square displacement. (Source: Reproduced from Ref. [106]).

contribution of mesopore diffusion to overall mass transfer in scenario (d) must therefore be expected to be notably larger than appearing from scenario (b) where the macropores and, hence, also the interface between the macropore and mesopore spaces are blocked. It is due to this reason that the diffusivity observed under condition (d) must be expected to be enhanced in comparison with the weighted mean of the diffusivities resulting under conditions (b) and (c). This is exactly also the outcome of the experiments shown in Fig. 12.

4. Conclusion

In the last few decades, PFG NMR has proved its unmatched capabilities for investigating molecular translational diffusion in complex systems, notably including nanoporous materials. It triggered a paradigm shift in our understanding on intracrystalline diffusion and provided novel insights into various limiting cases of diffusion in nanoporous materials. Convincing demonstrations of the applicability of the PFG NMR techniques to zeolites have impressively evidenced the importance of a close control of the key parameters and of the boundary conditions under which the experiments are performed. Only under such conditions, a valid correlation of the obtained data with physically meaningful phenomena and processes becomes attainable. Most recently, PFG NMR has in particular shown its enormous potential for probing diffusion in hierarchically organized porous materials. A significant enhancement of their quality features in comparison with conventional “monodisperse” porous materials is accompanied by a dramatic increase in the number of influencing parameters and, thus, in also the expenses of their measurement. Comprehensive knowledge on the governing phenomena of mass transfer, however, is quintessential for the optimum design and application of these materials. Combination of MAS and PFG NMR has reinforced the potential of NMR diffusometry by offering a new possibility for diffusion measurement with molecules of extremely low mobility which, so far, have been unobservable by PFG NMR. This paves the way for a new promising approach of NMR diffusometry to less mobile systems with increasing complexity.

Acknowledgement

Financial support by the Deutsche Forschungsgemeinschaft (DFG) and the Fonds der Chemischen Industrie is gratefully acknowledged. We appreciate stimulating discussions and manifold support by many colleagues, notably by Dieter Freude, Jürgen Haase and Rustem Valiullin in our immediate vicinity. J.K. cordially thanks the organizers of MRPM 14 for the invitation to a key note lecture which, in part, gave rise to this contribution.

Declarations of interest

None.

References

[1] Heitjans P, Kärger J. Diffusion in condensed matter: methods, materials, models. Berlin; New York: Springer; 2005. [965 pp.].
[2] Jost W. Diffusion in solids, liquids, gases. New York: Academic; 1960.
[3] Cussler EL. Diffusion: mass transfer in fluid systems. Cambridge: Cambridge University Press; 2009.
[4] Barrer RM, Fender BEF. The diffusion and sorption of water in zeolites—II. Intrinsic and self-diffusion. J Phys Chem Solid 1961;21(1):12–24.
[5] Ruthven DM, Derrah RI. Sorption in Davison 5 A molecular sieves. Can J Chem Eng 1972;50(6):743–7.
[6] Ruthven DM, Brandani S. Measurement of diffusion in microporous solids by macroscopic methods. In: Fraissard J, Conner CW, editors. Physical adsorption: experiment, theory, and applications. vol. 491. Dordrecht/Boston/London: Kluwer Academic Publishers; 1997. p. 261–96.
[7] Ruthven DM, Brandani S. Measurement of diffusion in porous solids by zero length column (ZLC) methods. In: Kanellopoulos NK, editor. Recent advances in gas separation by microporous ceramic membranes. Amsterdam: Elsevier; 2000. p. 187–212.
[8] Brandani S. The ZLC method for diffusion measurements. In: Zhou L, editor. Proceedings of the 4th Pacific Basin Conference on Adsorption Science and Technology. Singapore; Hackensack, NJ: World Scientific; 2007.
[9] Rees LVC, Shen D. Frequency-response measurements of diffusion of xenon in silicalite-1. J Chem Soc Faraday Trans 1990;86(21):3687–92.
[10] Yasuda Y, Mizusawa H, Kamimura T. Frequency response method for investigation of kinetic details of a heterogeneous catalyzed reaction of gases. J Phys Chem B 2002;106(26):6706–12.
[11] Wang Y, Levan MD. New developments in flow-through apparatus for measurement of adsorption mass-transfer rates by frequency response method. Adsorption 2005;11(1):409–14.
[12] Hayhurst DT, Paravar AR. Diffusion of C1 to C5 normal paraffins in silicalite.

Zeolites 1988;8(1):27–9.
[13] Bowen TC, Wyss JC, Noble RD, Falconer JL. Measurements of diffusion through a zeolite membrane using isotopic-transient pervaporation. Microporous Mesoporous Mater 2004;71(1):199–210.
[14] Caro J, Noack M, Kölsch P. Zeolite membranes: from the laboratory scale to technical applications. Adsorption 2005;11(3):215–27.
[15] Jobic H, Theodorou DN. Quasi-elastic neutron scattering and molecular dynamics simulation as complementary techniques for studying diffusion in zeolites. Microporous Mesoporous Mater 2007;102(1):21–50.
[16] Jobic H, Kolokolov DI, Stepanov AG, Koza MM, Ollivier J. Diffusion of CH4 in ZIF-8 studied by quasi-elastic neutron scattering. J Phys Chem C 2015;119(28):16115–20.
[17] Remi JCS, Lauerer A, Chmelik C, et al. The role of crystal diversity in understanding mass transfer in nanoporous materials. Nat Mater 2015;15:401.
[18] Heinke L, Kortunov P, Tzoulaki D, Kärger J. The options of interference microscopy to explore the significance of intracrystalline diffusion and surface permeation for overall mass transfer on nanoporous materials. Adsorption 2007;13(3):215–23.
[19] Kärger J, Ruthven DM. Diffusion in nanoporous materials: fundamental principles, insights and challenges. New J Chem 2016;40(5):4027–48.
[20] Kärger J, Binder T, Chmelik C, et al. Microimaging of transient guest profiles to monitor mass transfer in nanoporous materials. Nat Mater 2014;13:333.
[21] Hwang S, Parditka B, Cserháti C, et al. IR microimaging of direction-dependent uptake in MFI-type crystals. Chem Ing Tech 2017;89(12):1686–93.
[22] Stejskal EO, Tanner JE. Spin diffusion measurements: spin echoes in the presence of a time-dependent field gradient. J Chem Phys 1965;42(1):288–92.
[23] Tanner JE. Pulsed field gradients for NMR spin-echo diffusion measurements. Rev Sci Instrum 1965;36(8):1086–7.
[24] Price WS, Ide H, Arata Y. Self-diffusion of supercooled water to 238 K using PGSE NMR diffusion measurements. Chem A Eur J 1999;103(4):448–50.
[25] Price WS, Ide H, Arata Y, Söderman O. Temperature dependence of the self-diffusion of supercooled heavy water to 244 K. J Phys Chem B 2000;104(25):5874–6.
[26] Mills R. Self-diffusion in normal and heavy water in the range 1–45.deg. J Phys Chem 1973;77(5):685–8.
[27] McCall DW, Douglass DC, Anderson EW. Diffusion in liquids. J Chem Phys 1959;31(6):1555–7.
[28] Kärger J, Kočiřik M, Zikánová A. Molecular transport through assemblages of microporous particles. J Colloid Interface Sci 1981;84(1):240–9.
[29] Kärger J, Lenzner J, Pfeifer H, et al. NMR study of adsorbate self-diffusion in porous glasses. J Am Ceram Soc 1983;66(1):69–72.
[30] Kärger J, Ruthven DM. Diffusion in zeolites and other microporous solids. Wiley; 1992.
[31] Valiullin R. Diffusion NMR of confined systems. Cambridge: Royal Society of Chemistry; 2006.
[32] Knauss R, Schiller J, Fleischer G, Kärger J, Arnold K. Self-diffusion of water in cartilage and cartilage components as studied by pulsed field gradient NMR. Magn Reson Med 1999;41(2):285–92.
[33] Price WS. Recent advances in NMR diffusion techniques for studying drug binding. Aust J Chem 2003;56(9):855–60.
[34] Qiao Y, Galvosas P, Callaghan PT. Diffusion correlation NMR spectroscopic study of anisotropic diffusion of water in plant tissues. Biophys J 2005;89(4):2899–905.
[35] Kärger J, Ruthven DM, Theodorou DN. Diffusion in nanoporous materials. Wiley-VCH Verlag GmbH & Co. KGaA; 2012.
[36] Kärger J. Measurement of diffusion in zeolites—a never ending challenge? Adsorption 2003;9(1):29–35.
[37] Kärger J, Vasenkov S. Quantitation of diffusion in zeolite catalysts. Microporous Mesoporous Mater 2005;85(3):195–206.
[38] Kärger J. Diffusionsuntersuchung von Wasser an 13X- sowie 4A- und 5A-Zeolithen mit Hilfe der Methode der gepulsten Feldgradienten. Z Phys Chem 1971;248:27–41.
[39] Kärger J, Caro J. Interpretation and correlation of zeolitic diffusivities obtained from nuclear magnetic resonance and sorption experiments. J Chem Soc Faraday Trans 1 1977;73(0):1363–76.
[40] Kärger J. A study of fast tracer desorption in molecular sieve crystals. AIChE J 1982;28(3):417–23.
[41] Kärger J, Heink W. The propagator representation of molecular transport in microporous crystallites. J Magn Reson (1969) 1983;51(1):1–7.
[42] Callaghan PT. Principles of nuclear magnetic resonance microscopy. Oxford: Clarendon Press; 1991.
[43] Callaghan PT, Coy A, MacGowan D, Packer KJ, Zelaya FO. Diffraction-like effects in NMR diffusion studies of fluids in porous solids. Nature 1991;351:467.
[44] Chmelik C, Karger J. In situ study on molecular diffusion phenomena in nanoporous catalytic solids. Chem Soc Rev 2010;39(12):4864–84.
[45] Parravano C, Baldeschwieler JD, Boudart M. Diffusion of water in zeolites. Science 1967;155(3769):1535–6.
[46] Kärger J, Pfeifer H, Riedel E, Winkler H. Self-diffusion measurements of water adsorbed in NaY zeolites by means of NMR pulsed field gradient techniques. J Colloid Interface Sci 1973;44(1):187–8.
[47] D'Orazio F, Bhattacharja S, Halperin WP, Gerhardt R. Enhanced self-diffusion of water in restricted geometry. Phys Rev Lett 1989;63(1):43–6.
[48] Kärger J, Bülow M, Millward GR, Thomas JM. A phenomenological study of surface barriers in zeolites. Zeolites 1986;6(3):146–50.
[49] Kortunov P, Vasenkov S, Kärger J, et al. Diffusion in fluid catalytic cracking catalysts on various displacement scales and its role in catalytic performance. Chem Mater 2005;17(9):2466–74.
[50] Kärger J. Zur Bestimmung der diffusion in einem Zweibereichsystem mit Hilfe von gepulsten Feldgradienten. Ann Phys 1969;479(1–2):1–4.
[51] Kärger J. NMR self-diffusion studies in heterogeneous systems. Adv Colloid Interface Sci 1985;23:129–48.
[52] Kärger J, Pfeifer H, Heink W. Principles and application of self-diffusion measurements by nuclear magnetic resonance. In: Waugh JS, editor. Advances in magnetic and optical resonance. vol. 12. Academic Press; 1988. p. 1–89.
[53] Krutyeva M, Kärger J. NMR diffusometry with beds of nanoporous host particles: an assessment of mass transfer in compartmented two-phase systems. Langmuir 2008;24(18):10474–9.
[54] Waldeck AR, Kuchel PW, Lennon AJ, Chapman BE. NMR diffusion measurements to characterise membrane transport and solute binding. Prog Nucl Magn Reson Spectrosc 1997;30(1):39–68.
[55] Qiao Y, Galvosas P, Adalsteinsson T, Schönhoff M, Callaghan PT. Diffusion exchange NMR spectroscopic study of dextran exchange through polyelectrolyte multilayer capsules. J Chem Phys 2005;122(21):214912.
[56] Adalsteinsson T, Dong W-F, Schönhoff M. Diffusion of 77,000 g/mol dextran in submicron polyelectrolyte capsule dispersions measured using PFG-NMR. J Phys Chem B 2004;108(52):20056–63.
[57] Melchior J-P, Majer G, Kreuer K-D. Why do proton conducting polybenzimidazole phosphoric acid membranes perform well in high-temperature PEM fuel cells? Phys Chem Chem Phys 2017;19(1):601–12.
[58] Price WS. NMR studies of translational motion. Cambridge: Cambridge University Press; 2009.
[59] Nilsson M, Alerstam E, Wirestam R, Ståhlberg F, Brockstedt S, Lätt J. Evaluating the accuracy and precision of a two-compartment Kärger model using Monte Carlo simulations. J Magn Reson 2010;206(1):59–67.
[60] Haddar H, Li JR, Schiavi S. Adapting the Kärger model to account for finite diffusion-encoding pulses in diffusion MRI. IMA J Appl Math 2016;81(5):779–94.
[61] Niendorf T, Dijkhuizen RM, Norris DG, van Lookeren Campagne M, Nicolay K. Biexponential diffusion attenuation in various states of brain tissue: implications for diffusion-weighted imaging. Magn Reson Med 1996;36(6):847–57.
[62] Mulkern RV, Gudbjartsson H, Westin C-F, et al. Multi-component apparent diffusion coefficients in human brain†. NMR Biomed 1999;12(1):51–62.
[63] Clark CA, Le Bihan D. Water diffusion compartmentation and anisotropy at high b values in the human brain. Magn Reson Med 2000;44(6):852–9.
[64] Eriksson S, Elbing K, Söderman O, Lindkvist-Petersson K, Topgaard D, Lasič S. NMR quantification of diffusional exchange in cell suspensions with relaxation rate differences between intra and extracellular compartments. PLoS One 2017;12(5):e0177273.
[65] Cabrita EJ, Berger S, Bräuer P, Kärger J. High-resolution DOSY NMR with spins in different chemical surroundings: influence of particle exchange. J Magn Reson 2002;157(1):124–31.
[66] Gaede HC, Gawrisch K. Multi-dimensional pulsed field gradient magic angle spinning NMR experiments on membranes. Magn Reson Chem 2004;42(2):115–22.
[67] Pampel A, Zick K, Glauner H, Engelke F. Studying lateral diffusion in lipid bilayers by combining a magic angle spinning NMR probe with a microimaging gradient system. J Am Chem Soc 2004;126(31):9534–5.
[68] Fernandez M, Kärger J, Freude D, Pampel A, van Baten JM, Krishna R. Mixture diffusion in zeolites studied by MAS PFG NMR and molecular simulation. Microporous Mesoporous Mater 2007;105(1):124–31.
[69] Lauerer A, Kurzhals R, Toufar H, Freude D, Kärger J. Tracing compartment exchange by NMR diffusometry: water in lithium-exchanged low-silica X zeolites. J Magn Reson 2018;289:1–11.
[70] Kühl GH. Crystallization of low-solica faujasite ($SiO_2Al_2O_3$ ~ 2.0). Zeolites 1987;7(5):451–7.
[71] Schneider D, Toufar H, Samoson A, Freude D. 17O DOR and other solid-state NMR studies concerning the basic properties of zeolites LSX. Solid State Nucl Magn Reson 2009;35(2):87–92.
[72] Baerlocher C, McCusker LB, Olson DH. Atlas of zeolite framework types. Amsterdam: Elsevir; 2007.
[73] Beckert S, Stallmach F, Toufar H, Freude D, Kärger J, Haase J. Tracing water and cation diffusion in hydrated zeolites of type Li-LSX by pulsed field gradient NMR. J Phys Chem C 2013;117(47):24866–72.
[74] Freude D, Beckert S, Stallmach F, et al. Ion and water mobility in hydrated Li-LSX zeolite studied by 1H, 6Li and 7Li NMR spectroscopy and diffusometry. Microporous Mesoporous Mater 2013;172:174–81.
[75] Caro J, Hőcevar S, Kärger J, Riekert L. Intracrystalline self-diffusion of H2O and CH4 in ZSM-5 zeolites. Zeolites 1986;6(3):213–6.
[76] Mitra PP, Sen PN, Schwartz LM. Short-time behavior of the diffusion coefficient as a geometrical probe of porous media. Phys Rev B 1993;47(14):8565–74.
[77] Mitra PP, Sen PN, Schwartz LM, Le Doussal P. Diffusion propagator as a probe of the structure of porous media. Phys Rev Lett 1992;68(24):3555–8.
[78] Geier O, Snurr RQ, Stallmach F, Kärger J. Boundary effects of molecular diffusion in nanoporous materials: a pulsed field gradient nuclear magnetic resonance study. J Chem Phys 2004;120(1):367–73.
[79] Vasenkov S, Böhlmann W, Galvosas P, Geier O, Liu H, Kärger J. PFG NMR study of diffusion in MFI-type zeolites: evidence of the existence of intracrystalline transport barriers. J Phys Chem B 2001;105(25):5922–7.
[80] Vasenkov S, Kärger J. Evidence for the existence of intracrystalline transport barriers in MFI-type zeolites: a model consistency check using MC simulations. Microporous Mesoporous Mater 2002;55(2):139–45.
[81] Karwacki L, Kox MHF, Matthijs de Winter DA, et al. Morphology-dependent zeolite intergrowth structures leading to distinct internal and outer-surface molecular diffusion barriers. Nat Mater 2009;8:959.
[82] Stavitski E, Weckhuysen BM. Infrared and Raman imaging of heterogeneous catalysts. Chem Soc Rev 2010;39(12):4615–25.

[83] Liu Y, Meirer F, Krest CM, Webb S, Weckhuysen BM. Relating structure and composition with accessibility of a single catalyst particle using correlative 3-dimensional micro-spectroscopy. Nat Commun 2016;7:12634.
[84] Feldhoff A, Caro J, Jobic H, et al. Intracrystalline transport resistances in nanoporous zeolite X. Chemphyschem 2009;10(14):2429–33.
[85] Caro J, Bülow M, Jobic H, Kärger J, Zibrowius B. Molecular mobility measurement of hydrocarbons in zeolites by NMR techniques. In: Eley DD, Pines H, Weisz PB, editors. Advances in catalysis. vol. 39. Academic Press; 1993. p. 351–414.
[86] Jobic H, Schmidt W, Krause CB, Kärger J. PFG NMR and QENS diffusion study of n-alkane homologues in MFI-type zeolites. Microporous Mesoporous Mater 2006;90(1):299–306.
[87] Kondrashova D, Lauerer A, Mehlhorn D, et al. Scale-dependent diffusion anisotropy in nanoporous silicon. Sci Rep 2017;7:40207.
[88] Mitchell S, Pinar AB, Kenvin J, Crivelli P, Kärger J, Pérez-Ramírez J. Structural analysis of hierarchically organized zeolites. Nat Commun 2015;6:8633.
[89] Schwieger W, Machoke AG, Weissenberger T, et al. Hierarchy concepts: classification and preparation strategies for zeolite containing materials with hierarchical porosity. Chem Soc Rev 2016;45(12):3353–76.
[90] Coasne B. Multiscale adsorption and transport in hierarchical porous materials. New J Chem 2016;40(5):4078–94.
[91] Javier P-R, Danny V, Adriana B, Sònia A. Zeolite catalysts with tunable hierarchy factor by pore-growth moderators. Adv Funct Mater 2009;19(24):3972–9.
[92] Hartmann M. Hierarchical zeolites: a proven strategy to combine shape selectivity with efficient mass transport. Angew Chem Int Ed 2004;43(44):5880–2.
[93] Schneider D, Kondrashova D, Valiullin R, Bunde A, Kärger J. Mesopore-promoted transport in microporous materials. Chem Ing Tech 2015;87(12):1794–809.
[94] Schneider D, Mehlhorn D, Zeigermann P, Kärger J, Valiullin R. Transport properties of hierarchical micro–mesoporous materials. Chem Soc Rev 2016;45(12):3439–67.
[95] Laurent G, Maria M, Sharon M, Javier P-R. Superior mass transfer properties of technical zeolite bodies with hierarchical porosity. Adv Funct Mater 2014;24(2):209–19.
[96] Valiullin R, Kärger J, Gläser R. Correlating phase behaviour and diffusion in mesopores: perspectives revealed by pulsed field gradient NMR. Phys Chem Chem Phys 2009;11(16):2833–53.
[97] Zeigermann P, Naumov S, Mascotto S, Kärger J, Smarsly BM, Valiullin R. Diffusion in hierarchical mesoporous materials: applicability and generalization of the fast-exchange diffusion model. Langmuir 2012;28(7):3621–32.
[98] Valiullin R. Chapter two-diffusion in nanoporous host systems. In: Webb GA, editor. Annual reports on NMR spectroscopy. vol. 79. Academic Press; 2013. p. 23–72.
[99] Galarneau A, Guenneau F, Gedeon A, et al. Probing interconnectivity in hierarchical microporous/mesoporous materials using adsorption and nuclear magnetic resonance diffusion. J Phys Chem C 2016;120(3):1562–9.
[100] Mehlhorn D, Valiullin R, Kärger J, Cho K, Ryoo R. Intracrystalline diffusion in mesoporous zeolites. Chemphyschem 2012;13(6):1495–9.
[101] Mehlhorn D, Valiullin R, Kärger J, Cho K, Ryoo R. Exploring the hierarchy of transport phenomena in hierarchical pore systems by NMR diffusion measurement. Microporous Mesoporous Mater 2012;164:273–9.
[102] Heink W, Kärger J, Pfeifer H, Salverda P, Datema KP, Nowak A. Self-diffusion measurements of n-alkanes in zeolite NaCaA by pulsed-field gradient nuclear magnetic resonance. J Chem Soc Faraday Trans 1992;88(3):515–9.
[103] Jobic H, Kärger J, Krause C, et al. Diffusivities of n-alkanes in 5A zeolite measured by neutron spin echo, pulsed-field gradient NMR, and zero length column techniques. Adsorption 2005;11(1):403–7.
[104] Hu Y-S, Adelhelm P, Smarsly BM, Hore S, Antonietti M, Maier J. Synthesis of hierarchically porous carbon monoliths with highly ordered microstructure and their application in rechargeable lithium batteries with high-rate capability. Adv Funct Mater 2007;17(12):1873–8.
[105] Sonnenburg K, Adelhelm P, Antonietti M, Smarsly B, Nöske R, Strauch P. Synthesis and characterization of SiC materials with hierarchical porosity obtained by replication techniques. Phys Chem Chem Phys 2006;8(30):3561–6.
[106] Hwang S, Valiullin R, Haase J, Smarsly BM, Bunde A, Kärger J. Structural characterisation of hierarchically porous silica monolith by NMR cryo-porometry and -diffusometry. Diff Fundam 2017;29(6):1–7. online journal www.diffusion-fundamentals.org.
[107] Strange JH, Rahman M, Smith EG. Characterization of porous solids by NMR. Phys Rev Lett 1993;71(21):3589–91.
[108] Gane PAC, Ridgway CJ, Lehtinen E, et al. Comparison of NMR cryoporometry, mercury intrusion porosimetry, and DSC thermoporosimetry in characterizing pore size distributions of compressed finely ground calcium carbonate structures. Ind Eng Chem Res 2004;43(24):7920–7.
[109] Mitchell J, Webber JBW, Strange JH. Nuclear magnetic resonance cryoporometry. Phys Rep 2008;461(1):1–36.
[110] Kondrashova D, Valiullin R. Freezing and melting transitions under mesoscalic confinement: application of the Kossel–Stranski crystal-growth model. J Phys Chem C 2015;119(8):4312–23.
[111] Speedy RJ, Angell CA. Isothermal compressibility of supercooled water and evidence for a thermodynamic singularity at −45 °C. J Chem Phys 1976;65(3):851–8.
[112] Holten V, Bertrand CE, Anisimov MA, Sengers JV. Thermodynamics of supercooled water. J Chem Phys 2012;0136(9):094507.
[113] Kondrashova D, Dvoyashkin M, Valiullin R. Structural characterization of porous solids by simultaneously monitoring the low-temperature phase equilibria and diffusion of intrapore fluids using nuclear magnetic resonance. New J Phys 2011;13(1):015008.
[114] Nakanishi K, Shikata H, Ishizuka N, Koheiya N, Soga N. Tailoring mesopores in monolithic macroporous silica for HPLC. J High Resolut Chromatogr 2000;23(1):106–10.
[115] Stoeckel D, Kübel C, Hormann K, Höltzel A, Smarsly BM, Tallarek U. Morphological analysis of disordered macroporous–mesoporous solids based on physical reconstruction by nanoscale tomography. Langmuir 2014;30(30):9022–7.
[116] Meinusch R, Ellinghaus R, Hormann K, Tallarek U, Smarsly BM. On the underestimated impact of the gelation temperature on macro- and mesoporosity in monolithic silica. Phys Chem Chem Phys 2017;19(22):14821–34.
[117] Mehlhorn D, Kondrashova D, Küster C, et al. Diffusion in complementary pore spaces. Adsorption 2016;22(7):879–90.